ICSV19
Vilnius, Lithuania
July 08-12, 2012

SPATIAL AND TEMPORAL FILTERING FOR FEEDBACK CONTROL OF ROAD NOISE IN CARS

Jordan Cheer and Stephen J. Elliott

Institute of Sound and Vibration Research, University of Southampton, Southampton, SO17 1BJ, UK,
e-mail: j.cheer@soton.ac.uk

Active noise control systems offer a potential method of reducing the weight of passive acoustic treatment and, therefore, increasing vehicles' fuel efficiency. The widespread commercialisation of active noise control has, however, not been achieved partly due to the cost of implementation. To achieve cost-effective control of road noise, a feedback control strategy is presented which employs the array of microphones and the car audio loudspeakers common to a feedforward engine noise control system. The proposed system weights the contributions from the error microphones and the loudspeakers to increase the magnitude of the open-loop response over the bandwidth where noise attenuation is required, as in modal feedback control. This spatial filtering technique is combined with temporal filtering to further enhance the magnitude of the open-loop response over the targeted bandwidth and to compensate for the phase response of the control loudspeakers. The proposed feedback control system is shown to achieve reductions of up to 10 dB in the composite error signal, but only reduces the sum of the squared pressures by around 3 dB over a very narrow bandwidth.

1. Introduction

Noise in road vehicles has been widely acknowledged as a key factor governing their commercial success [1]. The reduction of both engine and road noise within the car cabin is currently achieved through the use of passive acoustic treatments such as structural damping and acoustic absorption [2]. However, over the last 20 years the application of active noise control to vehicles has been investigated [3] and, consequently, a wide variety of systems have been proposed to control both engine [3] and road noise [4]. This interest in active control solutions has recently been driven by the need to improve the fuel efficiency of vehicles through the use of more fuel-efficient engine designs and by reducing the vehicle's weight. Economical engine designs such as variable displacement, which usually operates by deactivating a number of cylinders, often result in an increased low frequency noise due to the use of a lower number of cylinders. Similarly, reducing the weight of a vehicle also results in increased low frequency noise. Low frequency noise is difficult to control using lightweight passive measures, and since active noise control systems are most effective at low frequencies and may be implemented within a car with relatively little increase in weight, they offer a convenient complementary solution. This is particularly true when the active noise control systems are integrated into the vehicle's electronic systems, for example, by employing the car audio loudspeakers [5].

The active control of engine noise using a feedforward control system was successfully demonstrated in the late 1980s [3] and a number of commercial systems have since been implemented. Feedforward control of engine noise is achieved by driving an array of loudspeakers with an engine

speed reference signal that is filtered adaptively so that the sum of squared pressures at an array of microphones is minimised. By integration with the car audio system, such a controller requires relatively little additional hardware and can therefore be implemented at little extra cost.

The active control of road noise has been demonstrated using a feedforward control system by Sutton *et al* [4], who report a reduction of around 7 dB in the A-weighted sound pressure level over a bandwidth of 100-200 Hz. However, to obtain suitable reference signals it is necessary to employ a number of accelerometers mounted to the vehicle's suspension and bodywork, which results in an expensive system that has, consequently, seen little commercial implementation.

As a result of the high cost of feedforward road noise control systems, interest has arisen in implementing road noise cancellation using a feedback system, as this avoids the need for separate reference sensors. Feedback control of road noise has been researched and implemented in a mass-production system by Honda [5]. This single channel feedback control system reduces the drumming noise associated with the first longitudinal mode of the car cabin at the front seats by 10 dB, whilst avoiding enhancements at the rear seats. To achieve global control of booming noise, a feedback controller based on modal control techniques widely employed in structural control [6] has been proposed by Cheer and Elliott [7]. This system employs an array of error sensors to enhance the open-loop response of the feedback controller at the targeted mode, whilst rejecting interference from other modes and thus reducing spillover. A global reduction of 8 dB in the acoustic potential energy in a car cabin sized rectangular enclosure is reported and this could be enhanced through the use of temporal filtering, as employed in a similar system used to control the sound field within an aircraft fuselage [8].

In this paper a feedback control system is presented which employs the spatial and temporal filtering techniques of modal control to achieve control of low frequency road noise in a vehicle cabin. The proposed control strategy uses the spatial and temporal filtering methods to enhance the open-loop response over the bandwidth where noise reduction is required and minimise the open-loop response at all other frequencies. The feedback control system is first described and the equations governing the stability and response of the controller are derived. A novel method of selecting the spatial transducer weightings is then discussed and a practical temporal filtering method is outlined. To investigate the performance of the feedback controller, a series of measurements of a small city car are conducted and employed to investigate both the controller's nominal performance and its robustness to plant uncertainties.

2. Feedback Control System

The proposed feedback control system has the same architecture as the modal feedback control strategies employed in [7, 8] and a block diagram of the system is presented in Fig. 1a. The feedback control system consists of M loudspeakers and L discrete error sensors, which may also be employed in a feedforward engine noise control system. A composite error signal, $e(j\omega)$, is generated through the weighted sum of the signals from the L discrete error microphones. This weighted sum is implemented via the $(L \times 1)$ vector of real, frequency independent, error sensor weightings, $\mathbf{w}_L$, and can be expressed in terms of the $(L \times 1)$ vector of pressures at the error sensors, $\mathbf{e}$, as,

$$e(j\omega) = \mathbf{w}_L^T \mathbf{e}(j\omega), \tag{1}$$

where ^{T} denotes the matrix transpose and the vector of pressures at the error sensors is given by the summation of the $(L \times 1)$ vectors of pressures due to the primary disturbance, $\mathbf{d}(j\omega)$, and the control sources, $\mathbf{y}(j\omega)$, so that

$$\mathbf{e}(j\omega) = \mathbf{d}(j\omega) + \mathbf{y}(j\omega) \tag{2}$$

$$= \mathbf{d}(j\omega) + \mathbf{G}(j\omega)\mathbf{u}(j\omega), \tag{3}$$

where $\mathbf{G}(j\omega)$ is the $(L \times M)$ matrix of plant responses and $\mathbf{u}(j\omega)$ is the $(M \times 1)$ vector of control signals. The composite error signal, $e(j\omega)$, is filtered by the negative feedback controller, $-H(j\omega)$, which incorporates the temporal filtering, to give the composite control signal,

$$u(j\omega) = -H(j\omega)e(j\omega). \tag{4}$$

The composite control signal is sent to the M loudspeakers, or secondary sources, via the $(M \times 1)$ vector of real, frequency independent source weightings, $\mathbf{w}_M$, which gives the vector of control signals as,

$$\mathbf{u}(j\omega) = \mathbf{w}_M u(j\omega). \tag{5}$$

Substituting equations 2 - 5 into equation 1 gives the composite error signal as,

$$e(j\omega) = \mathbf{w}_L^T \mathbf{d}(j\omega) - \mathbf{w}_L^T \mathbf{G}(j\omega)\mathbf{w}_M H(j\omega)e(j\omega). \tag{6}$$

If the scalar $\mathbf{w}_L^T \mathbf{d}(j\omega)$ is defined as the composite disturbance signal, $d(j\omega)$, and the scalar $\mathbf{w}_L^T \mathbf{G}(j\omega)\mathbf{w}_M$ is defined as the single-input-single-output (SISO) plant response, $G(j\omega)$, it can be seen that the complete feedback controller shown in Fig. 1a can be written as a single channel system, as shown in Fig. 1b, with the composite error signal given by,

$$e(j\omega) = d(j\omega) - G(j\omega)H(j\omega)e(j\omega). \tag{7}$$

Consequently, the frequency response of the sensitivity function, $S(j\omega)$, is given by,

$$S(j\omega) = \frac{e(j\omega)}{d(j\omega)} = \frac{1}{1 + G(j\omega)H(j\omega)} \tag{8}$$

and the open-loop response is given by,

$$G(j\omega)H(j\omega) = \mathbf{w}_L^T \mathbf{G}(j\omega)\mathbf{w}_M H(j\omega). \tag{9}$$

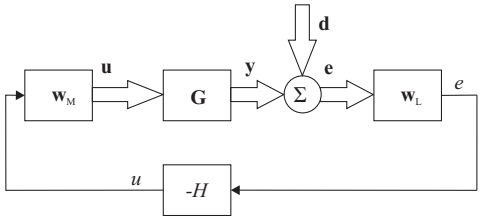

(a) Block diagram of the feedback controller employing spatial and temporal filtering.

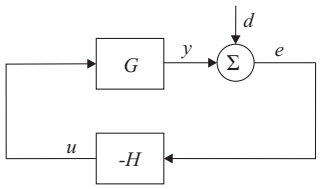

(b) Block diagram of the single channel representation of the feedback controller employing spatial and temporal filtering.

Figure 1: Feedback controller block diagrams.

In order to achieve good disturbance rejection the sensitivity function, given by equation 8, must be small, whilst to ensure the controller is robust to variations in the plant response the complementary sensitivity function should be small compared to unity [9]. Therefore, at frequencies where control is required, $G(j\omega)H(j\omega)$ should be large compared to unity, whilst at frequencies where control is not required, $G(j\omega)H(j\omega)$ should be kept small compared to unity. To achieve this using the controller presented in Fig. 1a, it is necessary to optimise both the spatial weighting vectors, $\mathbf{w}_L$ and $\mathbf{w}_M$, and the temporal filtering feedback controller, H.

2.1 Spatial Filtering

In the modal control system reported in [7] the transducer weightings, $\mathbf{w}_L$ and $\mathbf{w}_M$, can conveniently be determined based on the mode shape of the targeted mode and the relative positions of the transducers. However, in practical enclosures such as the small city car considered in the following application, the complexity of the structural-acoustic coupled system means that the transducer weightings are less straightforward to determine. A method of systematically optimising the transducer weightings when disturbance rejection is required over a specific frequency range is presented.

2.1.1 Sensor weighting optimisation

The aim of the spatial weighting vectors is to ensure that the sensitivity function is small at frequencies where disturbance rejection is required and close to unity elsewhere. To achieve this with respect to the sensor weighting it is necessary to maximise the response of the distributed sensor array, $\mathbf{w}_L^T\mathbf{G}(j\omega)$, over the frequency range where noise reduction is required, whilst minimising the response at all other frequencies. This can be expressed, for K discrete frequencies, as maximising the ratio,

$$C_L = \frac{\mathbf{w}_L^T \left(\sum_{k=c_1}^{c_2} \mathbf{G}(j\omega_k)\mathbf{G}^H(j\omega_k)\right) \mathbf{w}_L}{\mathbf{w}_L^T \left(\sum_{k=0}^{c_1-1} \mathbf{G}(j\omega_k)\mathbf{G}^H(j\omega_k) + \sum_{k=c_2+1}^{K} \mathbf{G}(j\omega_k)\mathbf{G}^H(j\omega_k)\right) \mathbf{w}_L}. \tag{10}$$

where c_1 and c_2 are the upper and lower bounds of the bandwidth targeted for disturbance rejection. Defining the summation over the targeted and rejected bandwidths as,

$$\mathbf{T}_L = \sum_{k=c_1}^{c_2} \mathbf{G}(j\omega_k)\mathbf{G}^H(j\omega_k), \tag{11}$$

and

$$\mathbf{R}_L = \sum_{k=0}^{c_1-1} \mathbf{G}(j\omega_k)\mathbf{G}^H(j\omega_k) + \sum_{k=c_2+1}^{K} \mathbf{G}(j\omega_k)\mathbf{G}^H(j\omega_k), \tag{12}$$

allows equation 10 to be written more concisely as,

$$C_L = \frac{\mathbf{w}_L^T\mathbf{T}_L\mathbf{w}_L}{\mathbf{w}_L^T\mathbf{R}_L\mathbf{w}_L}. \tag{13}$$

The maximisation of the ratio C_L can be cast as a constrained optimisation problem in which $\mathbf{w}_L^T\mathbf{T}_L\mathbf{w}_L$ is maximised with the constraint that $\mathbf{w}_L^T\mathbf{R}_L\mathbf{w}_L$ is held constant with a value c. The cost function to be maximised can be expressed using the method of Lagrange multipliers as [10],

$$J_L = \mathbf{w}_L^T\mathbf{T}_L\mathbf{w}_L + \lambda\left(\mathbf{w}_L^T\mathbf{R}_L\mathbf{w}_L - c\right), \tag{14}$$

where λ is the real positive Lagrange multiplier. Since the sensor weightings are constrained to be real, it can be shown that the cost function to be maximised is [11],

$$J_L = \mathbf{w}_L^T\Re\{\mathbf{T}_L\}\mathbf{w}_L + \lambda\left(\mathbf{w}_L^T\Re\{\mathbf{R}_L\}\mathbf{w}_L - c\right). \tag{15}$$

Differentiating this cost function with respect to $\mathbf{w}_L$, equating to zero and rearranging gives,

$$\mathbf{w}_L = -\lambda\Re\{\mathbf{T}_L\}^{-1}\Re\{\mathbf{R}_L\}\mathbf{w}_L. \tag{16}$$

To maximise the cost function, J_L, the vector of sensor weightings must thus be the eigenvector of the matrix $\Re\{\mathbf{T}_L\}^{-1}\Re\{\mathbf{R}_L\}$ corresponding to its largest eigenvalue.

2.1.2 Source weighting optimisation

The vector of real source weightings, $\mathbf{w}_M$, can also be optimised by maximising the response of the distributed array of secondary sources over the targeted frequency bandwidth, whilst minimising its response at other frequencies. This can be expressed, for K discrete frequencies, as maximising the ratio,

$$C_M = \frac{\sum_{k=c_1}^{c_2} \mathbf{w}_M^T \mathbf{G}^H(j\omega_k)\mathbf{G}(j\omega_k)\mathbf{w}_M}{\sum_{k=0}^{c_1-1} \mathbf{w}_M^T \mathbf{G}^H(j\omega_k)\mathbf{G}(j\omega_k)\mathbf{w}_M + \sum_{k=c_2+1}^{K} \mathbf{w}_M^T \mathbf{G}^H(j\omega_k)\mathbf{G}(j\omega_k)\mathbf{w}_M}, \tag{17}$$

where the response of the distributed array is given by $\mathbf{G}(j\omega)\mathbf{w}_M$. Defining the summation over the targeted and rejected bandwidths as,

$$\mathbf{T}_M = \sum_{k=c_1}^{c_2} \mathbf{G}^H(j\omega_k)\mathbf{G}(j\omega_k), \tag{18}$$

and

$$\mathbf{R}_M = \sum_{k=0}^{c_1-1} \mathbf{G}^H(j\omega_k)\mathbf{G}(j\omega_k) + \sum_{k=c_2+1}^{K} \mathbf{G}^H(j\omega_k)\mathbf{G}(j\omega_k), \tag{19}$$

allows equation 17 to be written more concisely as,

$$C_M = \frac{\mathbf{w}_M^T \mathbf{T}_M \mathbf{w}_M}{\mathbf{w}_M^T \mathbf{R}_M \mathbf{w}_M}. \tag{20}$$

The maximisation of the ratio C_M can once again be cast as a constrained optimisation where, in this case, $\mathbf{w}_M^T \mathbf{T}_M \mathbf{w}_M$ is maximised with the constraint that $\mathbf{w}_M^T \mathbf{R}_M \mathbf{w}_M$ is held constant with a value c. Following the method presented in Section 2.1.2 it can be shown that the optimal source weightings are given as,

$$\mathbf{w}_M = -\lambda \Re\{\mathbf{T}_M\}^{-1} \Re\{\mathbf{R}_M\} \mathbf{w}_M, \tag{21}$$

and the cost function J_M is maximised if the vector of source weightings is equal to the eigenvector of the matrix $\Re\{\mathbf{T}_M\}^{-1}\Re\{\mathbf{R}_M\}$ corresponding to its largest eigenvalue.

2.2 Temporal Filtering

The performance of the feedback controller depicted in Fig. 1a can be further improved by specifying a frequency dependent feedback controller H. This can been achieved using a number of different controller design methods [9]. However, a simple temporal filtering method employing an all-pass filter for phase-compensation will be investigated herein following the formulation presented in [12]. The total response of the feedback controller is thus defined as,

$$H(j\omega) = gH_{AP}(j\omega), \tag{22}$$

where g is a frequency independent gain and $H_{AP}(j\omega)$ is the frequency response of the all-pass filter.

To ensure maximal control over the targeted bandwidth, it is necessary for the phase of the open-loop response in this bandwidth to be close to 0 radians or multiples thereof. This can be achieved through phase-compensation, which has traditionally been implemented using lead-lag compensation. Herein, however, an all-pass filter is tuned to give a phase response of 0 radians at the frequency of maximum disturbance level, ω_c, which is inherently within the control bandwidth. The frequency response of an all-pass filter is given by,

$$H_{AP}(j\omega) = \frac{j\omega - z}{j\omega + p}, \tag{23}$$

where z and p are the pole and zero of the all-pass filter and must be equal to ensure filter stability [13]. The required value of z to give a phase response of 0 radians at ω_c is,

$$z = \frac{j\omega_c}{\tan\left(\frac{\pi+\theta_{GH}(j\omega_c)}{2}\right)}, \tag{24}$$

where $\theta_{GH}(j\omega_c) = \angle \mathbf{w}_L^T \mathbf{G}(j\omega_c)\mathbf{w}_M H_{BP}(j\omega_c)$.

3. Application to Road Noise Control in Cars

To demonstrate the performance of the proposed feedback active noise control system a series of measurements have been conducted in a small city car to determine both the plant response, $\mathbf{G}$, and the disturbance produced at the error sensors, $\mathbf{d}$, when the car is driven at 50 km/h on a pavè road surface. The investigated control system consists of the four standard car audio loudspeakers – 2 positioned in the front doors and 2 positioned adjacent to the rear seats – and eight electret microphones positioned in the nominal corners of the car, which are consistent with the microphone locations required for a feedforward engine noise control system [7]. A further set of eight electret microphones have been positioned at the four car headrests to separately assess the controller's performance. The bandwidth targeted for control is between 80 and 180 Hz, where there is a significant peak in the disturbance spectrum, due to a structural resonance in the vehicle and the frequency of maximum disturbance level is 117 Hz.

Using the plant responses measured with a driver and a passenger occupying the cabin, the spatial source and sensor weightings have been calculated and the open-loop response of the feedback controller is presented in Fig. 2 for the system with and without temporal filtering and a gain that has been adjusted in each case so that the maximum enhancement in the composite error signal is 6 dB. From the Bode plot in Fig. 2a it can be seen that in both control systems $|GH|$ is largest over the targeted bandwidth, which is indicated by dashed vertical lines. It can also be seen that the temporal filtering reduces the phase-lag in the targeted bandwidth and facilitates an increase in the feedback gain. This can also be seen from the Nyquist plot in Fig. 2b, where the frequency of maximum disturbance level is also shown.

Figure 3a shows the power spectral density of the composite error signal, formed from the weighted sum of the microphone signals, both before and after control. Using the feedback controller employing spatial and temporal filtering, reductions of about 10 dB are predicted in the targeted frequency range of 80 to 180 Hz, with enhancements of less than 6 dB, at about 70 Hz for example. Unfortunately, when the effects of this feedback controller are calculated on the sum of the squared error signals, E_p, which is deinfed as $E\left[\mathbf{e}(j\omega)^H \mathbf{e}(j\omega)\right]$, the reductions are considerably less, with only about a 3 dB reduction being achieved in a very narrow range of frequencies around 100 Hz. Close examination of the matrix of measured plant responses highlights that over the targeted bandwidth there are a number of discrete resonances, which are excited in a complex way by a number of uncorrelated sources of noise. The single channel feedback control system is only able to control one of these resonances and, therefore, although the internal, composite error signal can be attenuated, the effect on the sum of the squared pressures is marginal, since the multitude of uncontrolled acoustic and structural resonances then dominates.

4. Conclusions

A feedback control system employing spatial and temporal filtering has been described and its performance has been investigated when applied to the active control of road noise in a small city car. The controller, which is based on modal feedback strategies, has been described and it is

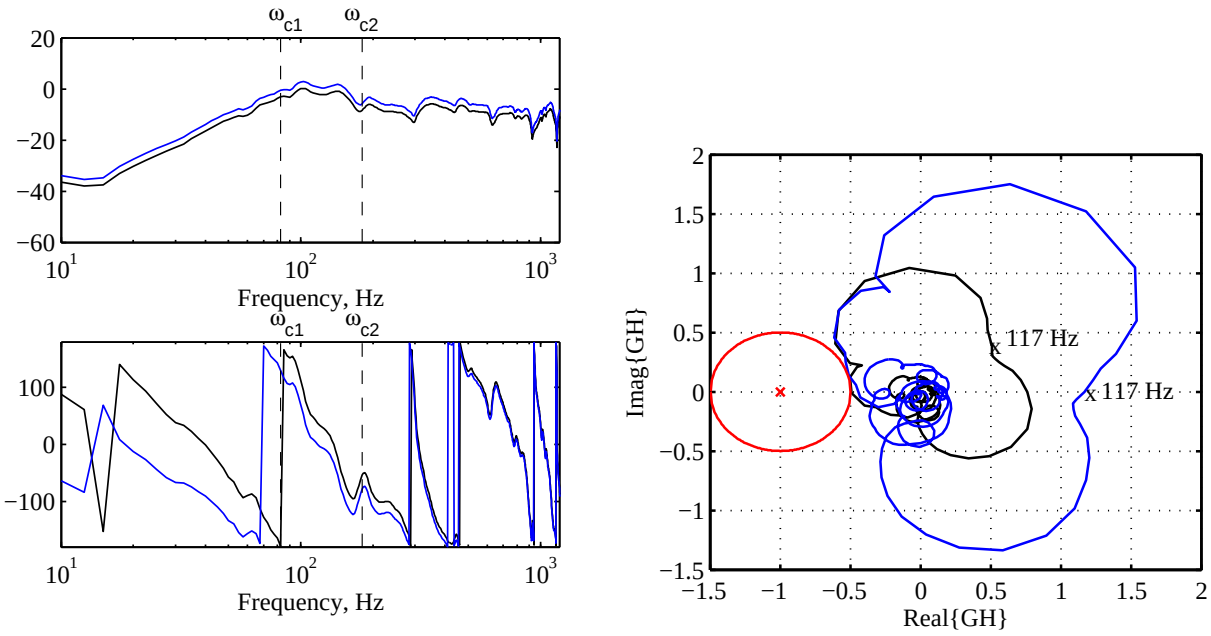

(a) Bode plot of the open-loop responses.

(b) Nyquist plot of the open-loop responses.

Figure 2: The predicted open-loop response of the feedback controller employing spatial filtering (—) and that employing spatial and temporal filtering (—).

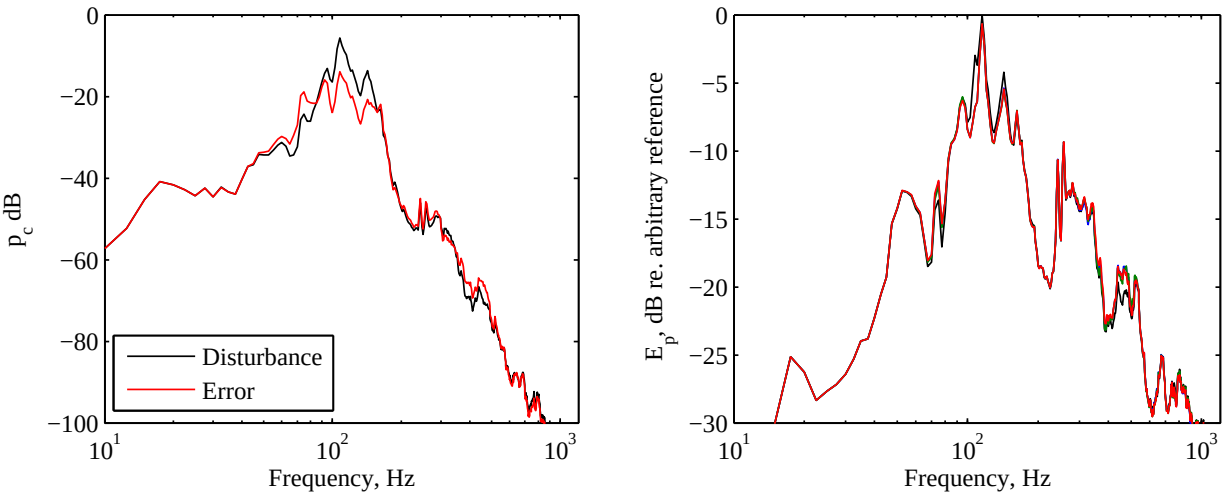

(a) The A-weighted composite disturbance and error signals

(b) The A-weighted acoustic potential energy estimate before and after control.

Figure 3: The predicted performance of the feedback controller employing eight spatially weighted microphones and four spatially weighted car audio loudspeakers and a temporal filter. The level in each case is shown before control (—) and for the nominal, driver + passenger, plant response (—).

shown that despite employing a number of error sensors and sources it behaves as a SISO system. A novel method of optimising the transducer weightings to achieve control of the composite error signal over a specific bandwidth has been detailed and a simple temporal filtering method previously employed in modal feedback control is described. The performance of the proposed controller has been evaluated through offline predictions, using plant responses and disturbance data measured in a small city car. The offline simulations predict reductions of up to 10 dB in the composite error signal over the targeted bandwidth. Unfortunately, however, this is predicted to make very little difference to the sum of the squared microphone signals, which is a measure of the global pressure level in the vehicle. This is believed to be due to the fact that the enclosure's response over the targeted bandwidth has contributions from a number of acoustic and structural resonances, which are excited in a complex way by a number of uncorrelated noise source, and the single channel controller cannot independently control each of these resonances. In vehicle enclosures, such as estate cars or station wagons, where a well separated acoustic mode occurs the presented system may, therefore, achieve significant levels of global control. However, in order to provide a more general solution that may be able to control several dominant resonances, a multichannel extension of the presented control strategy is currently being investigated.

Acknowledgements

This research was funded by the "European Green City Car, Co2ntrol" project, which is part of the FP7 programme.

REFERENCES

[1] X. Wang, Rationale and history of vehicle noise and vibration refinement, in *Vehicle Noise and Vibration Refinement* (X. Wang, ed.), Woodhead Publishing, Cambridge, 3–17, (2010).

[2] D. Vigé, Vehicle interior noise refinement - cabin sound package design and development, in *Vehicle Noise and Vibration Refinement* (X. Wang, ed.), Woodhead Publishing, Cambridge, 286–317, (2010).

[3] S. J. Elliott, I. M. Stothers, P. Nelson, M. A. McDonald, D. C. Quinn, and T. J. Saunders, The active control of engine noise inside cars, in *Proceedings of INTER-NOISE 88*, **2**, Poughkeepsie, New York, 987–990, (1988).

[4] T. J. Sutton, S. J. Elliott, M. A. McDonald, and T. J. Saunders, Active control of road noise inside vehicles, *J. Noise Control Eng.*, **42**, 137–146, (1994).

[5] H. Sano, T. Inoue, A. Takahashi, K. Terai, and Y. Nakamura, Active control system for low-frequency road noise combined with an audio system, *IEEE Trans. Speech, Audio Process.*, **9**, 775–763, (2001).

[6] L. Meirovitch, *Dynamics and control of structures*, Wiley-Interscience publication, New York, (1990).

[7] J. Cheer and S. J. Elliott, The effect of structural-acoustic coupling on the active control of sound in vehicles, in *Proc. Eurodyn 2011*, (2011).

[8] S. A. Lane, R. L. Clark, and S. C. Southward, Active control of low frequency modes in an aircraft fuselage using spatially weighted arrays, *J. Vib. and Acoust.*, **122**, 227–233, (2000).

[9] S. J. Elliott, *Signal Processing for Active Control*, Academic Press, London, (2001).

[10] R. Fletcher, *Practical Methods of Optimization*, 2nd ed. John Wiley & sons, New Jersey, (2000).

[11] P. A. Nelson, A. R. D. Curtis, S. J. Elliott, and A. J. Bullmore, The minimum power output of free field point sources and the active control of sound, *J. Sound and Vib.*, **116**(3), 397–414, (1987).

[12] J. B. Bisnette, A. K. Smith, J. S. Vipperman, and D. D. Budny, Active noise control using phase-compensated, damped resonant filters, *J. Vib. and Acoust.*, **128**(2), 148–155, (2006).

[13] P. Regalia, S. Mitra, and P. Vaidyanathan, The digital all-pass filter: a versatile signal processing building block, *Proc. of the IEEE*, **76**, 19 –37, (1988).